Simulation and Optimization of Conductor Structural Parameters of Free-space Hall-Effect Current Sensor

Jianhai Qiu, Ji-Gou Liu and Quan Zhang
ChenYang Technologies GmbH & Co. KG
Markt Schwabener Str. 8, 85464 Finsing, Germany
Email: jigou.liu@chenyang-ism.com

Jianzhong Lin
University of Shanghai for Science and Technology, USST
Jungong Rd. 516, 200093 Shanghai, China
Email: Linjz@usst.edu.cn

***Abstract* –In this paper, simulation is done to optimize the conductor structural parameters of a new free space current sensor by using Ansoft Maxwell software. These parameters are conductor shape, gap between conductor and Hall-effect sensor, cross-section geometry and length of conductor pins, respectively. The optimized parameters are implemented in a new free-space current sensor with using a Hall-effect element. Experimental results show that the sensitivity of the new designed current sensor is relatively stable, the linearity can be controlled within ±0.6%, and the total measuring error is less than 3.0%, which is lower than that of the integrated current sensor, for instance ACS756.**

Keywords –Free-Space Hall Effect Current Sensor, Conductor Sructural Optimization, Magnetic field simulation

I. INTRODUCTION

In industry, increasing numbers of occasions need to trace the current for monitoring, controlling and protecting devices, such as automotive, household appliances, generators, and motor drives. Therefore current sensors find more and more applications.

There are many current sensors, including Hall-effect current sensors, current transformers, shunt resistors etc. Compared with the current transformers and shunt resistors, Hall-effect current sensors are preferred because of their wide measuring range, better linearity and accuracy, good isolation between the input and output [1].The traditional Hall current sensors are divided as open loop current sensor and closed loop current sensor, in which a magnetic core with a high permeability is used to concentrate the magnetic flux generated by the primary current so that the sensors can get a high sensitivity [2,3,4]. However, in some applications where space is limited and sensitivity and accuracy are not dominantly concerned, such as a low cost servo driver, free-space current sensors can be used thanks to its simple structure, small size and low cost.

As shown in Fig. 1, free-space current sensor is a coreless Hall-effect current sensor, and composed only of a primary current carrying conductor, a Hall-effect element and an amplifier circuit. The primary current carrying conductor generates a magnetic field which varies with the current. The magnetic field can be detected by the Hall element, the output of which is processed by the amplifier circuit. In this way one can monitor the current passing though the conductor.

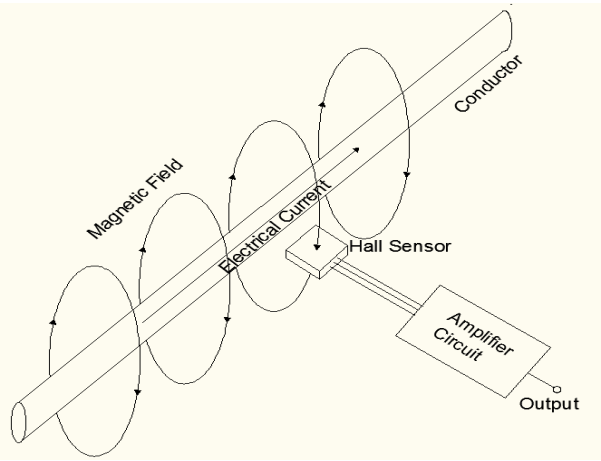

Fig. 1. Structure of free-Space Hall-effect current sensor

Nevertheless, there are several problems should be noted when designing a free-space Hall current sensor. Firstly, free-space current sensor is highly sensitive to the position error between the Hall sensor and current conductor. Secondly, the Hall element cannot get a high magnetic field generated by the primary current under test. The sensitivity and the accuracy of the sensor are highly limited by these facts [1].

The goal of this paper is to improve the sensitivity and linearity of free-space current sensor by optimizing the structural parameters, such as conductor shape, gap between conductor and Hall-effect element, cross-section geometry, length of conductor pins. Optimization is done by magnetic field simulation by using Ansoft Maxwell software. The simulation model is proved by experiments. The optimized parameters are applied to a new free-space current sensor with using a Hall-effect element.

II. SIMULATION AND OPTIMIZATION

The goal of magnetic field simulation by using Ansoft Maxwell is to optimize the magnetic flux density that the Hall element senses under different conditions. Fig. 2 shows the simulation model, the main characteristics of which are as follows:

1) Current excitation loads on the two ends of the electric conductor.
2) Adaptive meshing, the number of the elements is not more than 30,000.
3) The nonlinear residual of the model is controlled within 0.01.

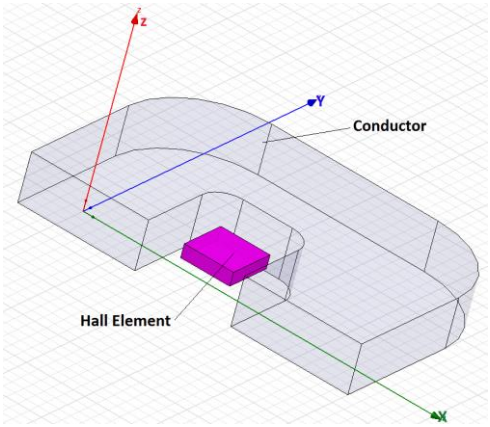

Fig. 2. Simulation model

A. Conductor Shape

According to the Biot-Savart's Law, the magnetic flux density increases with the increasing current. Based on the Ampere Circuital Theorem, for a straight conductor of circular-section, the magnetic flux density around it can be expressed as:

$$B = \frac{\mu_0 I}{2\pi r} \quad (1)$$

Where μ_0 is the permeability of vacuum, r is the distance from an arbitrary point outside the conductor to the centerline of the conductor.

Apparently, if two or more electric conductors are under test, the target point has a larger magnetic field. Therefore the conductor could have a pattern of polygon. Considering other factors such as ease installation and small sensor size, a U-shaped conductor is preferred, as shown in Fig. 3.

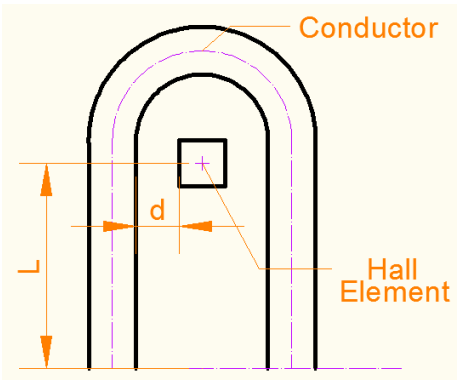

Fig. 3. Conductor Structure under Simulation

In Fig. 3 L is the distance from the end of the pins to the sensing center of the Hall element, defined as the length of the pins, and d is the distance of the gap between the Hall element and the conductor.

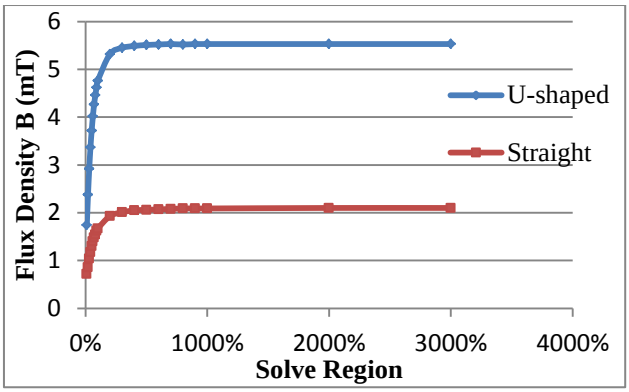

Fig. 4. Magnetic flux density generated by a U-shaped conductor and a straight conductor at d=2mm and I=50A.

Fig. 4 shows the magnetic flux density generated by a U-shaped conductor and a straight conductor at the same gap d=2mm and under supplying the same current I=50A. It can be found that the magnetic flux density generated by the U-shaped conductor is much higher than that by the straight conductor. The improvement factor is about 2.6. Therefore the sensitivity under using U-shaped conductor is higher than that of using straight conductor.

B. Gap size between Hall Element and Conductor

Based on the scheme shown in Fig. 3 and (1), it can be concluded that the smaller the gap d is, the larger the magnetic field at the target point where the Hall element locates. However, for the new free-space current sensor that this paper concerns, the current carrying conductor should be electrically isolated from the Hall element with a galvanic isolation of 2.5 kV, therefore the gap size needs to be optimized.

According to the Paschen's Law, for uniform electric field, the air gap breakdown voltage can be estimated by using the following empirical equation [5]:

$$U_s = 24.4\delta d + 6.53\sqrt{\delta d} \quad \text{(kV)} \quad (2)$$

with δ as the relative air density, used to characterize the change in barometric pressure P, and d the gap size in cm. Apparently, equation (2) is symmetrically respect to the two variables, δ and d. Supposing the relative air density δ equal 1, the breakdown voltage is the function of the gap size d, as shown in Fig. 5.

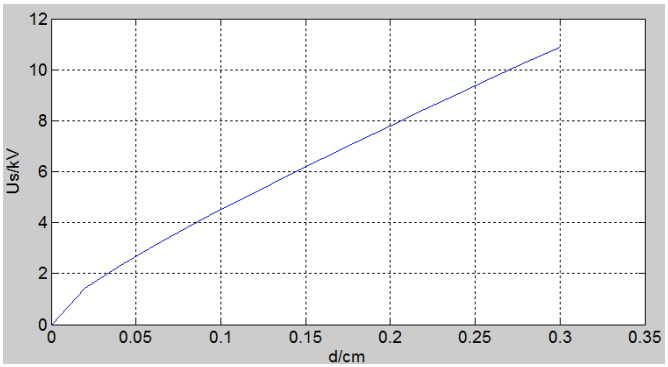

Fig. 5. Relationship between the breakdown voltage and the gap d (under δ = 1)

It is important to note that this is obtained on the basis of a uniform electric field. If the excitation electric field is non-uniform, the air gap breakdown voltage will decrease. The extent of the decline is associated with the uniformity of electric field. In fact, most of the electric field is non-uniform. In order to guarantee a galvanic isolation of 2.5 kV, a margin coefficient can be used to keep the air from breakdown by a non-uniform electric field. For a margin coefficient of 1.6, the gap size *d* can be 0.86mm, see Fig. 5.

A gap size of 2 mm is used in following analyses as it makes the experiments easy to realize.

C. Cross-section Geometry of Conductor

The magnetic field generated by an electric conductor depends on its cross-section [6, 7]. In order to maximize the magnetic flux density where the Hall element positions it is necessary to optimize the conductor cross-section.

Fig. 6 shows five kinds of cross-sectional geometry, four of them have a same cross-section area of 12.56mm^2 (see Fig.6 a, b, c, d), another one has a square cross-section whose area is 16mm^2(see Fig. 6 e).

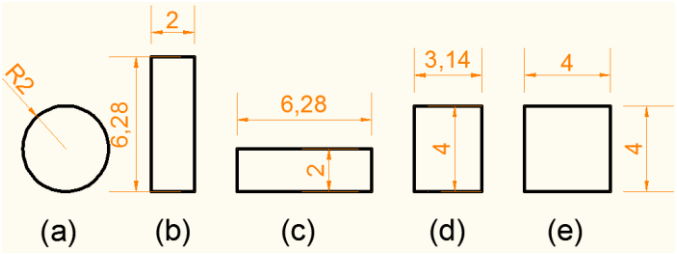

Fig. 6. Cross-section geometry of electric conductor

Fig. 7 and Table 1 show the results of the magnetic field simulation of the cross-sections when *d*=2mm, *I*=50A, *L*=2.05mm.

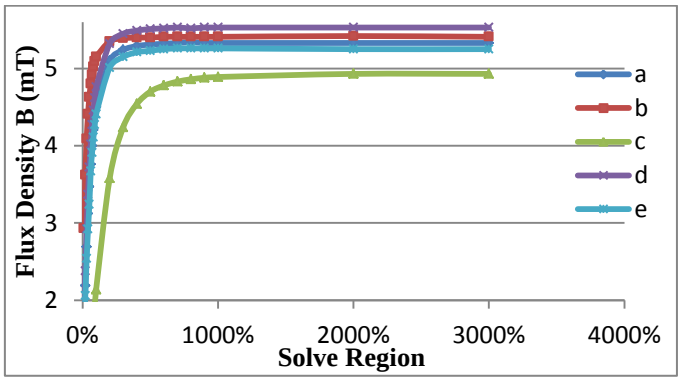

Fig. 7. Magnetic field simulation results with different cross-section geometries

TABLE 1. MAXIMUM MAGNETIC FLUX DENSITY *B*

Cross-section	(a)	(b)	(c)	(d)	(e)
B (mT)	5.33	5.41	4.93	5.53	5.25

From the simulation results one can conclude that:

- The larger the current density or the smaller the distance between the Hall element and conductor centerline, the bigger the magnetic flux density.
- The magnetic field of a rectangular cross-section conductor which is slightly narrower than a circular-section conductor (see Fig. 6 d) is the largest. Nevertheless, the difference is not significant.

Considering easy manufacturing, installation and low production cost etc., a circular cross-section conductor (see Fig. 6 a) is appreciated. The section radius depends on the measuring range of the current sensor.

D. Conductor Length

For a free-space current sensor, the magnetic field generated by the external input pins could affect the flux density of the target point. In order to ignore this influence the conductor length should be optimized by simulation. In the simulation the length *L* changes from 6mm to 24mm, under *d*=2mm, the conductor diameter 2*R*2=Ø1.3mm. The simulation results are given as relative deviation:

$$\varepsilon_{L_{i+1}-L_i} = \frac{B_{L_{i+1}} - B_{L_i}}{B_{L_i}} \times 100\%, i = 1,2,3 \qquad (3)$$

As shown in Fig. 8, the relative deviation decreases with increasing length of the conductor pins. This is because the influence of the magnetic field generated by the part near the end of the conductor pins weakens gradually as *L* increases.

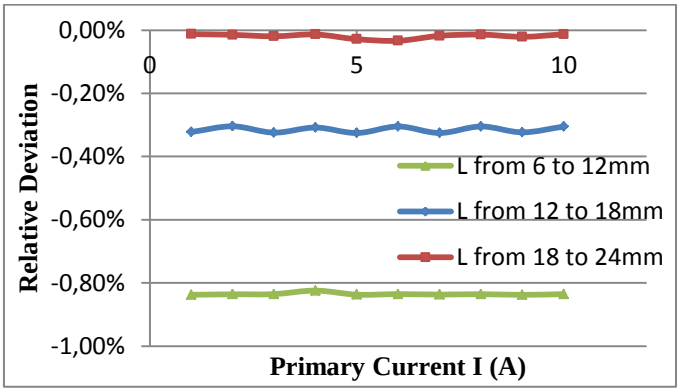

Fig. 8. Relative deviation of the magnetic field simulation results under different length L

It can be concluded that the influence is really small when the conductor length $L \geq 24$mm.

III. EXPERIMENTAL VERIFICATION

The simulation model is verified by using the simulation results of a straight cable *H07V-K 1*25 mm*^{2} and a circular-section, U-shaped conductor with diameter Ø1.3mm, in comparison with their experimental results. The Gauss meter CYHT201, whose accuracy is ±2.0% for DC magnetic field measurement [8], is used to measure the magnetic field density of target point.

A. *Sraight Cable H07V-K 1*25 mm^2*

Fig. 9 shows a measuring system of current flowing in a straight cable. Experiments are repeat done for ten times as the position of Gauss meter probe changes along the axis of cable. The magnetic field density as function of current is shown in Fig. 10.

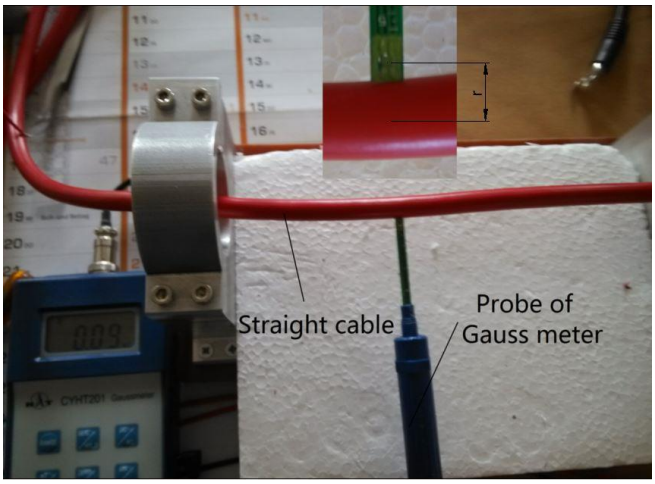

Fig. 9. Measuring system for straight cable

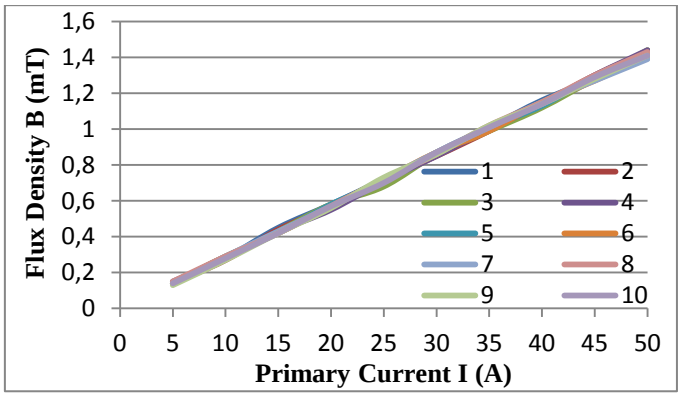

Fig. 10. Measured magnetic field density for straight cable as function of current

As the cable is straight, magnetic field can be calculated by (1). In this example, r is the sum of the cable radius and the distance from the top of the Hall probe of Gauss meter CYHT201 to the center of the Hall chip, r=7.15mm, see Fig. 9. The relative deviations are given as:

$$\begin{cases} \varepsilon_{s-m} = \frac{B_s - B_m}{B_m} \times 100\% \\ \varepsilon_{s-t} = \frac{B_s - B_t}{B_t} \times 100\% \\ \varepsilon_{m-t} = \frac{B_m - B_t}{B_t} \times 100\% \end{cases} \quad (4)$$

Where B_s, B_m and B_t are the simulated, measured and theoretical values of the magnetic flux density of the straight cable, respectively.

Fig. 11 shows the relative error between the simulation, measured and theoretical values according to (4). B_m is the average of each measured magnetic field density. All relative deviations are not higher than ±3% when current changes from 5A to 50A. And the relative deviations between simulation and theoretical values are quite small, less than ±0.4%.

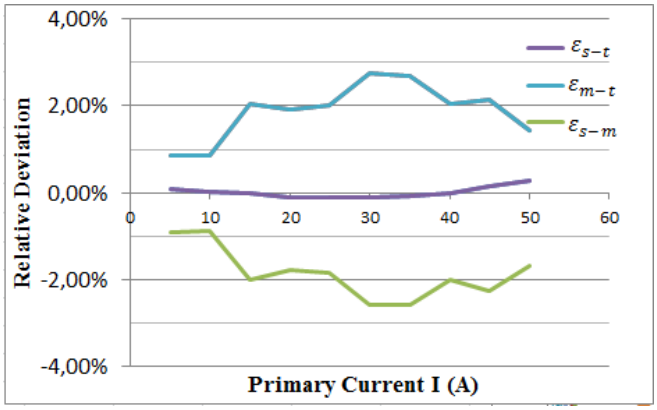

Fig. 11. Relative deviation between the simulation, measured and theoretical values

B. *U-shaped Conductor of Diameter Ø1.3mm*

Firstly, it should be noted that the cross-section area of the conductor used in this experiment is relatively small. It heats remarkably when the current goes high. Due to the thermal drift of the Hall probe of the Gauss meter, the measured values of magnetic flux density will deviate from the true values. The deviations increase with the increasing current.

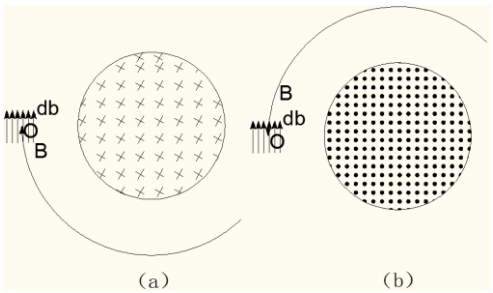

Fig. 12. Magnetic field generated by electric conductor in which a bidirectional current flows

As shown in Fig. 12, the measuring error due to thermal drift is seen as an interferential magnetic field. Its magnetic flux density, $db(I)$, varies with the current I. The current flows into the terminal (Fig. 12a) and flows out from the terminal (Fig. 12b). According to the Ampere's rule, the magnetic flux density is given as:

$$\begin{cases} B_{ma}(I) = B(I) + db(I) \\ B_{mb}(I) = -B(I) + db(I) \end{cases} \quad (5)$$

By calculating the modulus on the both sides of (5) as:

$$\begin{cases} |B_{ma}(I)| = B(I) + db(I) \\ |B_{mb}(I)| = B(I) - db(I) \end{cases} \quad (6)$$

The modulus of the magnetic flux density at point O can be determined by the average value:

$$|B_O| = \frac{|B_{ma}(I)|+|B_{mb}(I)|}{2} = B(I) \quad (7)$$

Based on (5)-(7), the way to measure the magnetic flux density can be optimized.

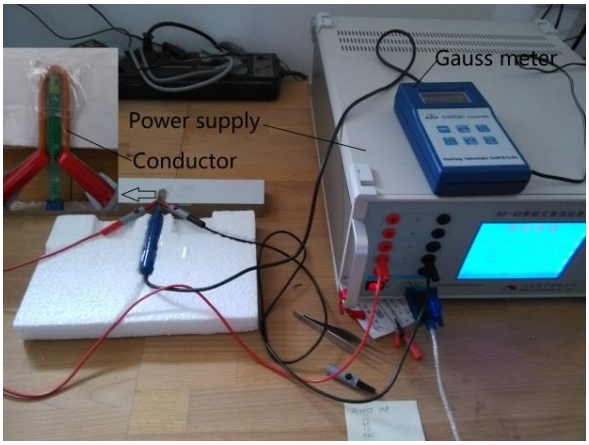

Fig. 13. Measuring system for U-shaped conductor

The measuring system for U-shaped conductor is shown in Fig. 13. Fig. 14 shows the magnetic flux density at the target point generated by a conductor of Ø1.3mm as function of current. It can be seen that the green curve obtained by using the above measuring method is very approximate to the simulation result. The relative deviations between the simulation and measured results of each experiment are not higher than ±3%, see Fig.15.

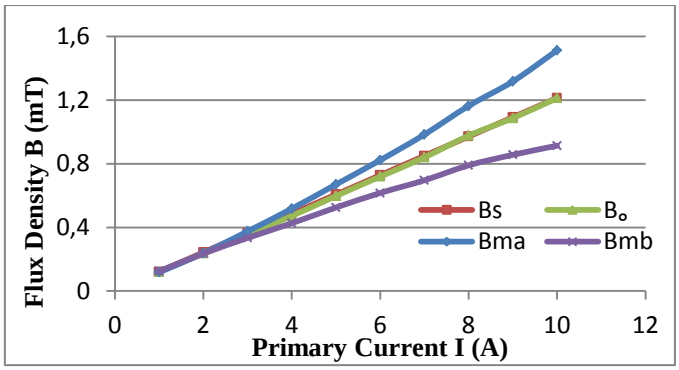

Fig. 14. Magnetic flux density of target point as function of current

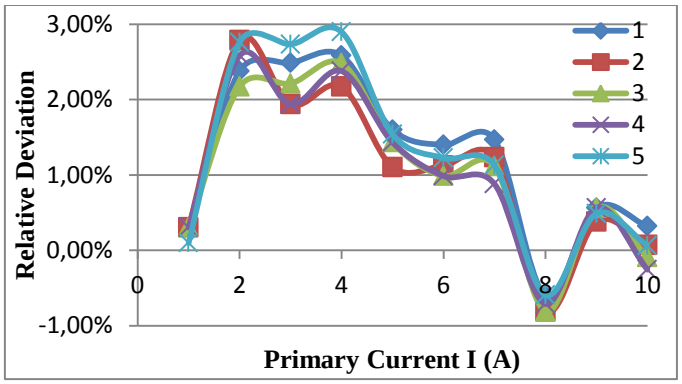

Fig. 15. Relative deviation between the simulation and measured values

IV. APPLICATION

The above simulation and optimization results are used to a new designed free-space Hall-effect current sensor. And the test model is shown in Fig. 16.

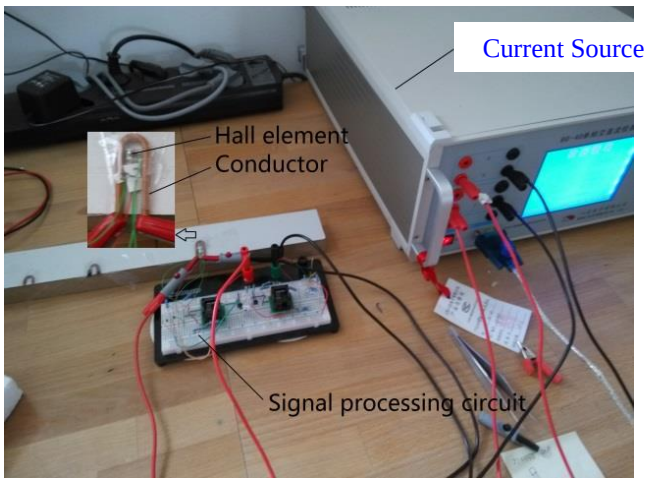

Fig. 16. Test system for development of new current sensor

Considering the current carrying capacity, a conductor of diameter Ø1.3mm is preferred for the experimental range 0-10A. Fig. 17 shows the sensitivity of the current sensor, which has been tested for ten times, under d=2mm and L=24mm. The red point represents the average sensitivity. The relative deviations between the measured values and the average are within ±1.0%, see Fig. 18.

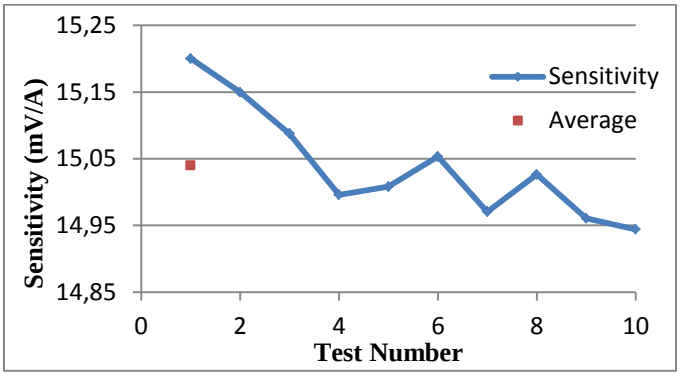

Fig. 17. Sensitivity of the free-space current sensor

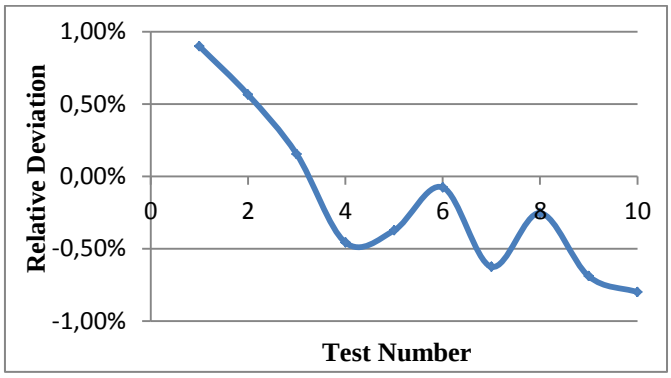

Fig. 18. Relative deviation between the measured sensitivities and the average

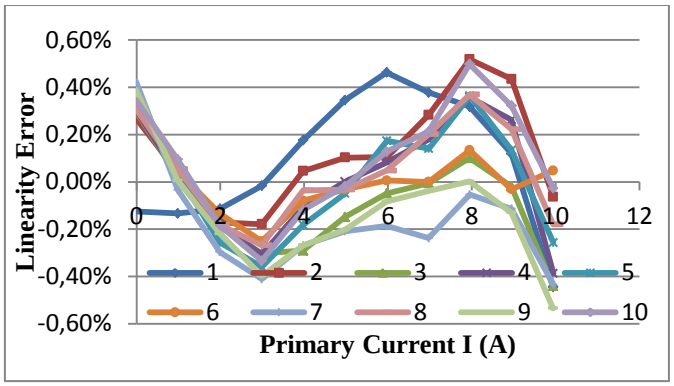

Fig. 19. Linearity error of the current sensor

Fig. 19 shows the linearity error of the current sensor. The linearity is repeat measured for 10 times. The linearity error of the current sensor is lower than ±0.6%.

TABLE 2. ACCURACY OF THE SENSOR

Accuracy at 25℃				
Zero Offset error	**Half-scale Current**	**Linearity**	**Repeatability**	**Total Output error**
±0.2%	±0.3%	±0.6%	±1.5%	±2.6%

Table 2 gives the accuracy of the free-space sensor at ambient temperature of 25℃. The total output error is ±2.6%. A basic accuracy of ±3.0% is realizable for mass-production. It is a better accuracy than that of the integrated current sensor ACS756, in which a ferrite core is built [9].

Furthermore, the above results are based on gap size *d* of 2mm. For mass-production a gap size of 1.0mm should be used. In this case the accuracy will be further improved thanks to the higher magnetic flux density generated by the conductor.

V. CONCLUSIONS

In this paper, simulations have been done to optimize the structural parameters of the conductor in a new free-space Hall-effect current sensor. The simulation model has been verified by the experiments. And the parameters optimized are used in the current sensor. From the results one can draw the following conclusions:

- The magnetic flux density generated by a U-shaped conductor is much higher than that by a straight conductor.
- A gap size of about 1.0mm can guarantee the sensor to have an electrical isolation voltage of 2.5kV.
- A circular cross-section conductor is appreciated thanks to its low cost, easy availability and relatively high magnetic flux density generated by it.
- The influence of the magnetic field generated by the part near the end of the conductor pins is gradually reduced by increasing length L. And it can be ignored if L is greater than 24mm.
- The sensitivity of the new designed free-space current sensor is relatively stable and the average sensitivity is about 15mv/A.
- The linearity error of the new designed free-space current sensor can be controlled within ±0.6%.
- A basic accuracy of ±3.0% is realizable for free-space current sensors under using the optimized parameters of the conductor.

VI. REFERENCES

[1] E. Ramsden, "Hall Effect Sensors – Theory and Application". Elsevier Inc., Amsterdam, London, New York etc., 2006.

[2] Y. Wang et al., "Split core closed loop Hall effect current sensors and applications". *Int. Exhibition and Conference for Power Electronics, Intelligent Motion, Power Quality*, Nuremberg, Germany, 8-10 May, 2012.

[3] G. Gokmen, K. Tuncalp, "The design of a Hall effect current transformer and examination of the linearity with real time parameter estimation". *Electron. and Elect. Eng.*, vol. 101, no. 5, pp. 3-8, Jun. 2010.

[4] Ho-Gi et al., "Coreless current sensor for automotive inverters decoupling cross-coupled field". *J. of Power Electron.*, vol. 9, no. 1, Jan. 2009.

[5] Z.-C. Zhou, "Breakdown characteristics of the air gap," in *High Voltage Engineering*, 3nd. Beijing, China:CEP Press,2007, pp. 38-44.

[6] J. T. Conway, "Trigonometric integrals for the magnetic field of the coil of rectangular cross section," *IEEE Trans. Magn.*, vol. 42, no. 5, pp.1538-1548, May., 2006.

[7] S. I. Babic and C. Akyel, "An improvement in the calculation of the magnetic field for an arbitrary geometry coil with rectangular cross section," *Int. J. Numerical Modeling*, vol. 18, no. 6, pp. 493-504, Oct., 2005.

[8] ChenYang Technologies GmbH & Co. KG. *Gaussmeter/Teslameter CYHT201* [Online]. Availabe: http://www.chenyang.de.

[9] Allegro MicroSystems. LLC. (2006). *Fully integrated, Hall effect-based linear current sensor IC with 3 kVRMS voltage isolation and a low-resistance current conductor* [Online]. Availabe: http://www.allegromicro.com/en/Products/Current-Sensor-ICs/Fifty-To-Two-Hundred-Amp-Integrated-Conductor-Sensor-ICs/ACS756.aspx